The Balance of Forward and Backward Hippocampal Sequences Shifts Across Behavioral States

Andrew M. Wikenheiser and A. David Redish*

ABSTRACT: Place cell firing patterns in the rat hippocampus are often organized as sequences. Sequences falling within cycles of the theta (6–10 Hz) local field potential (LFP) oscillation represent segments of ongoing behavioral trajectories. Sequences expressed during sharp wave ripple (SWR) complexes represent spatial trajectories through the environment, in both the same direction as actual trajectories (forward sequences) and in an ordering opposite that of behavior (backward sequences). Although hippocampal sequences could fulfill unique functional roles depending on the direction of the sequence and the animal's state when the sequence occurs, quantitative comparisons of sequence direction across behavioral and physiological states within the same experiment, employing consistent methodology, are lacking. Here, we used cross-correlation and Bayesian decoding to measure the direction of hippocampal sequences in rats during active behavior, awake rest and slow-wave sleep. During pretask sleep, few sequences were detected in either direction. Sequences within theta cycles during active behavior were overwhelmingly forward. Sequences during quiescent moments of behavior were both forward and backward, in equal proportion. During postbehavior sleep, sequences were again expressed in both directions, but significantly more forward than backward sequences were detected. The shift in the balance of sequence direction could reflect changing functional demands on the hippocampal network across behavioral and physiological states. © 2012 Wiley Periodicals, Inc.

KEY WORDS: replay; decoding; hippocampus; sharp wave

INTRODUCTION

The hippocampus is an important component of the brain's learning, memory and decision-making systems (O'Keefe and Nadel, 1978; Cohen and Eichenbaum, 1993; Redish, 1999). Hippocampal pyramidal neurons fire in a location-dependent manner as rats move through the environment (O'Keefe and Dostrovsky, 1971; O'Keefe, 1976).

The hippocampus exhibits two dominant network states, differentiated by unique local field potential (LFP) signatures (Vanderwolf, 1971; O'Keefe and Nadel, 1978). During attentive behavior, the hippocampal LFP exhibits strong, 6–10 Hz theta oscillations (Vanderwolf, 1969; O'Keefe and Nadel, 1978; Buzsaki et al., 1983). Within cycles of the theta rhythm, sequences of place cell spiking represent segments of the subject's ongoing movement trajectory (O'Keefe and Recce, 1993; Skaggs et al., 1996; Dragoi and Buzsaki, 2006; Foster and Wilson,

2007). The functional role of theta sequences is unknown, but the spatial extent represented within a single sequence is affected by behavior (Maurer et al., 2011; Gupta et al., in press), and theta sequences are not simply a consequence of phase precession (Foster and Wilson, 2007; Schmidt et al., 2009; Redish and Ekstrom, in press).

Less attentive behaviors such as awake rest, grooming, and slow-wave sleep are accompanied by disorganized, large amplitude fluctuations of the LFP (Vanderwolf, 1971; O'Keefe and Nadel, 1978). During the LIA (large, irregular activity) network state, the hippocampal LFP is punctuated by sharp-wave ripple (SWR) complexes, population bursts of spiking that produce distinctive LFP oscillations (O'Keefe and Nadel, 1978; Buzsaki et al., 1983; Buzsaki, 1989). Trajectories encoded by place cells during behavior reoccur in spiking within SWRs, during both off-line states such as sleep (Wilson and McNaughton, 1994; Skaggs and McNaughton, 1996; Nadasdy et al., 1999; Kudrimoti et al., 1999), and during active states, such as awake immobility (Foster and Wilson, 2006; Jackson et al., 2006; Diba and Buzsaki, 2007; Gupta et al., 2010). Because SWR-associated sequences are expressed on a timescale appropriate for synaptic plasticity, such firing patterns could function in preserving transient memory traces induced by behavior as more permanent representations stored in synaptic weights, (Marr, 1971; Buzsaki, 1989; Sutherland and McNaughton, 2000; Hoffmann and McNaughton, 2002; Jadhav and Frank, 2009). Models of memory consolidation are based on this principle (Hasselmo, 1993; Redish and Touretzky, 1998; Sutherland and McNaughton, 2000).

Recent findings, however, challenge the notion that hippocampal sequences function principally in consolidation. Sequences replayed by the hippocampus can diverge substantially from behavior (Davidson et al., 2009; Karlsson and Frank, 2009; Gupta et al., 2010), and are influenced by cognitive factors such as novelty (Hirase et al., 2001; Cheng and Frank, 2008), learning (Jackson et al., 2006) and reinforcement (Singer and Frank, 2009). Backward sequences (representations of trajectories in the direction opposite of locomotion; Foster and Wilson, 2006; Davidson et al., 2009; Gupta et al., 2010) further challenge the consolidation hypothesis, as reverse sequences would lead to storage of episodic events in the incorrect order.

Disrupting patterned reactivation during SWRs produces dissociable behavioral effects depending on whether the disruption is performed during on-line (Jadhav et al., 2012) or off-line (Girardeau et al., 2009; Ego-Stengel and Wilson, 2010) states.

Although backward and forward sequences might fulfill unique functions, it is unknown whether or how the balance of backward and forward events varies across behavioral and physiological states. Previous studies of hippocampal sequences have tended to examine sequences within a single behavioral condition or network state. Thus, comparing the balance of forward and backward sequences across these conditions necessarily involves comparisons across groups of animals, experimental conditions and analytical techniques for detecting and quantifying hippocampal firing sequences.

Here, we examined the direction of sequences during sleep, active behavior and quiescent pauses in behavior within the same experiment, using cross-correlation and Bayesian decoding approaches to analyze sequences.

MATERIALS AND METHODS

Subjects and Behavior

Data was collected from three male rats (Fisher-Brown Norway hybrids; Harlan, Indianapolis, IN) aged 6–14 months. Rats were food deprived to no less than 85% of their free-feeding weight; water was always freely available in the home cage. All procedures were conducted according to National Institutes of Health guidelines for animal care and approved by the University of Minnesota IACUC. Rats performed a decision-making task in which they ran clockwise laps around an elevated circular track (diameter = 80 cm) and waited for food pellets (45 mg; Research Diets, New Brunswick, NJ) dispensed from automated feeders (Med-Associates, St. Albans, VT) at each of three equidistant sites positioned around the maze. Subjects performed the task for 30 min daily. To ensure that subjects ran only clockwise laps, during training sessions (before electrode implantation) attempts at reversing direction were manually blocked. However, the narrow track width made it difficult for subjects to turn around, and attempts to do so were rare during training, and did not occur during recording sessions. Data from 28 sessions (10 from rat 1, 10 from rat 2, 8 from rat 3) are analyzed here.

Surgery and Data Collection

Rats were implanted with 12-tetrode hyperdrives (Kopf, Tujunga, CA) targeting the CA1 region of the right hippocampus (-3.8 mm anteroposterior, 3.0 mm lateral from bregma). Surgical procedures have been described in detail elsewhere (Jackson et al., 2006; Wikenheiser and Redish, 2011). Tetrodes were advanced slowly over the course of several days until electrophysiological signatures and depth estimates indicated they had reached the CA1 pyramidal cell layer. Neural data was recorded by a 64-channel Neuralynx Cheetah system (Bozeman, MT), and an overhead camera tracked subject position via LEDs on the headstage. Data collection and preprocessing was as described previously (Jackson et al., 2006; Wikenheiser and Redish, 2011). Each recording session began by recording 10–15 min of neural data as subjects rested on a platform placed in the center of the track. Then, subjects performed the behavioral task for thirty minutes. After task performance, subjects were returned to the center platform and 20–30 min of neural data were recorded as they rested. The mean session ensemble size was 39.3 cells (range, 28–62 cells). Cell yields were similar for all subjects (mean ensemble size rat 1: 47.2 cells; rat 2: 52.7 cells; rat 3: 36.4 cells).

Cross-Correlation

For the cross-correlation analysis, data were divided into four epochs. During the prerun epoch, the rat rested on a platform placed in the center of the track for 10–15 min prior to task performance. During run epochs, the rat performed the behavioral task for 30 min. The run-LIA epoch was defined as times when the z-scored ratio of theta to delta (2–4 Hz) oscillatory power (Csicsvari et al., 1999; Jackson et al., 2006) fell below 0. The run-theta epoch consisted of times when the z-scored theta-delta ratio exceeded 0.5. Finally, during the post-run epoch the rat rested on the same platform as the pre-run epoch for 20–30 min. To isolate periods of slow-wave sleep during the prerun and postrun epochs, we followed inclusion criteria outlined in previous experiments (Skaggs and McNaughton, 1996; Nadasdy et al., 1999; Kudrimoti et al., 1999; Lee and Wilson, 2002; Lansink et al., 2009). Data were restricted to times when the theta-delta ratio was below 0 and movement speed was <2 cm/s. Based on these criteria, 39.3% of prerun data and 57.0% of postrun data were included for analysis. However, given that slow-wave sleep and awake immobility share many behavioral and electrophysiological characteristics, we cannot exclude the possibility that the prerun and postrun epochs contain periods of awake quiescence in addition to slow-wave sleep. We computed pair-wise cross-correlations of units with at least one place field during task performance. Place fields were identified as in Wikenheiser and Redish (2011). The cross-correlation was computed separately for each epoch, and spanned a 1 s window with 1ms bin size. Examples of cross-correlograms across all epochs are shown in Figure 1.

Figure 2 was constructed by binning the distance separating cell pair place fields and averaging the correlograms in each spatial bin. Cells exhibiting multiple place fields (22.3%) were assigned to the spatial bin of the field with the greatest mean firing rate (Diba and Buzsaki, 2007). Each spatial bin was z-scored and smoothed by convolution with a Gaussian kernel ($\sigma = 50$ ms). The peak correlation value in each temporal bin was marked with a blue dot to facilitate visual inspection. To quantify the balance of forward and backward correlation strength (Fig. 3), we compared the mean intensity of pixels in forward (southwest and northeast) and backward (northwest and southeast) quadrants of correlograms with a ranksum test.
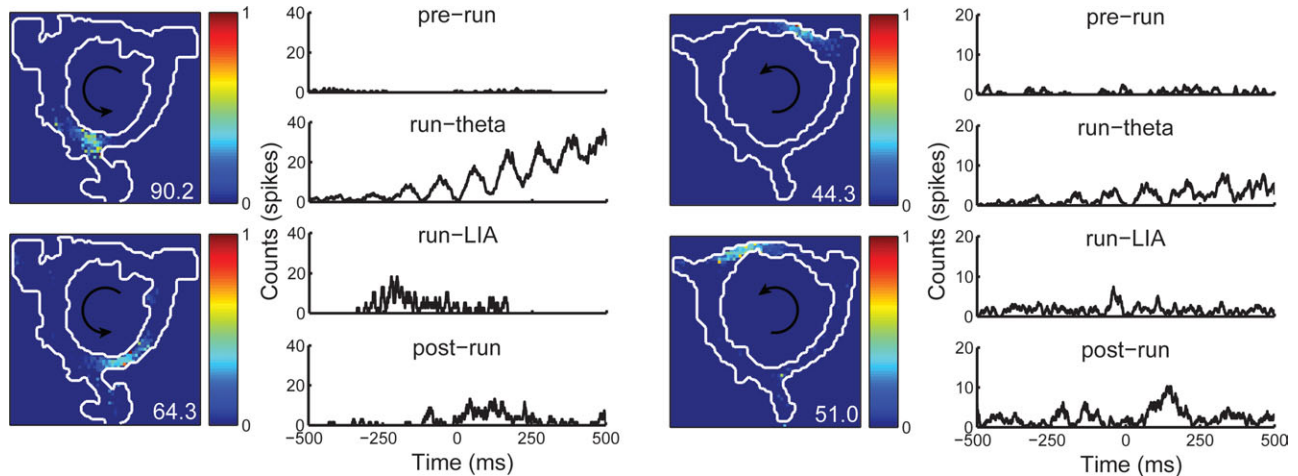
FIGURE 1.   Examples of spatial firing rate maps and cross-correlograms for two cell pairs. Firing rate maps are normalized for ease of visual comparison (peak rate of the cell is indicated in the bottom-right corner of each rate map). During the prerun epoch, little coordinated spiking is present. In contrast, during the run-theta epoch a strong, theta-modulated correlation is apparent. During the run-LIA and postrun epochs, peaks in the correlograms consistent with forward and backward-ordered sequential activity are present. [Color figure can be viewed in the online issue, which is available at wileyonlinelibrary.com.]

This analysis was performed on the raw (i.e., not smoothed or z-scored) cross-correlograms.

To examine the effect exerted by units with multiple place fields, we performed the cross-correlation analysis described above excluding multifield cells. The general pattern of correlations (Fig. 2) and the statistical conclusions of the analysis (Fig. 3) were unaffected by exclusion of cells with multiple fields. We performed another variant of the cross-correlation analysis in which correlograms of multifield cell pairs were duplicated and sorted into bins corresponding to all possible separations between the cell pair's fields. Again, the visual pattern of the correlations and the statistical findings of the quantification were unchanged (data not shown).

Bayesian Decoding of Ripple Events and Theta Cycles

To detect ripple events, the LFP recorded from the pyramidal cell layer was band-pass filtered at ripple frequency (140–220 Hz) and the power in this band was estimated via the Hilbert transform. As in previous studies (e.g., Karlsson and Frank 2009), candidate ripple events were defined as 150 ms windows centered on times when ripple power exceeded a threshold (one standard deviation above the baseline value). We chose a lower ripple threshold than some previous studies to err on the side of decoding many putative events and used a bootstrapping procedure (described below) to assess the significance of each
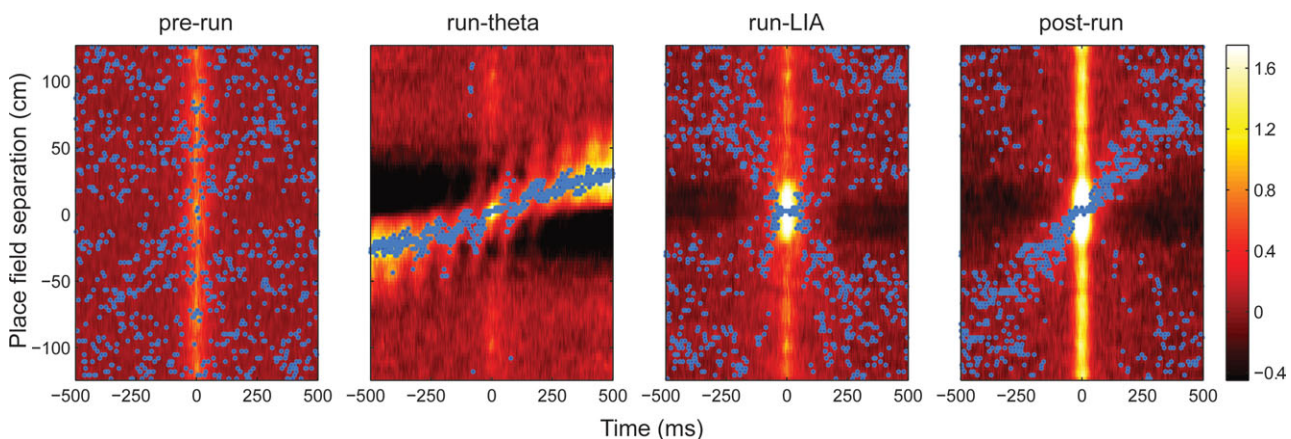

FIGURE 2.   Cross-correlograms of cell pairs exhibiting place fields during behavior. The color scale is equal for all panels (more intense colors indicate greater correlation strength). The maximum value in each 1-ms time bin is marked with a blue dot. Correlations were unpatterned preceding behavior (pre-run). During the run-theta epoch, forward correlations due to the nearby place fields (large band of heightened correlation across the entire window) and due to sequences within theta cycles (smaller bands spaced at ~120-ms intervals) are visible. Correlation patterns during the run-LIA epoch suggest both forward and backward sequences, as evidenced by bands of activity along both diagonals. During the postrun epoch, heightened activity is again present along both diagonals. [Color figure can be viewed in the online issue, which is available at wileyonlinelibrary.com.]
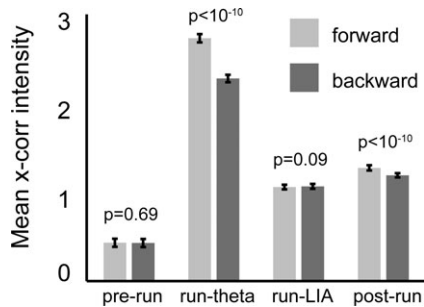
FIGURE 3. To quantify the strength of correlations in each direction, we compared pixels in the quadrants of correlograms corresponding to forward and backward sequences. Correlation strength did not differ for the prerun and run-LIA epochs. However, forward correlations were significantly stronger during the run-theta and post-run conditions.

event's sequence content. Overlapping events were concatenated. Only events in which at least 3 neurons fired a total of at least five spikes were included for analysis. To isolate times of sleep during pre- and post-periods, only events surrounded by at least 30 s of little or no motion (movement speed <2 cm/s) and mean theta-delta ratio <0 were included. To ensure that theta sequences were not misclassified as ripple events within the run-LIA epoch, candidate events were included only if the rat's average speed during the event was <2 cm/s and the average theta-delta ratio during the event was <0.

We used one-step, Bayesian decoding (Zhang et al., 1998) to estimate spatial locations represented by ensemble spiking. Given spike counts from each cell in the ensemble, this method computes the posterior probability of the ensemble representing each position in space; with the simplifying assumptions that cells' firing is independent of other cells in the ensemble and that spike counts follow a Poisson distribution, Bayesian decoding provides a statistically justified method of estimating locations represented by an ensemble of place cells. We decoded spiking in 10 ms time windows using a uniform spatial prior, resulting in a posterior probability distribution across 64 spatial bins ($\sim$ 4 cm each). Posterior distributions were normalized to sum to one, and we calculated the decoded position for each time step as the circular mean of the posterior probability distribution (that is, the vector sum with the central angle of each bin weighted by the amount of probability it contained). Within candidate events, only time steps containing at least one spike were decoded. In the cross-correlation analysis, units exhibiting multiple fields were classified with respect to the field with the greatest average firing rate. Bayesian decoding, however, correctly assigns probability weighted by the firing rate of cells across the entire maze. Thus, cells with multiple firing fields did not interfere with decoding of sequential representations. To detect sequences, we computed the cumulative sum of the difference between successive decoded positions. Forward sequences were characterized by positive differences, so their cumulative sum had a positive slope. The opposite was true of backward sequences. We performed a linear regression on the cumulative sum of differences from each decoded event, and used the bootstrap procedure of Karlsson and Frank

(2009) to identify statistically significant sequences. Of 24,240 candidate ripples (across all sessions), 6,796 (28%) were deemed significant. Considered by epoch, 5.9% of prerun candidates, 28.3% of run-LIA candidates and 25.4% of postrun candidates met the criterion for significance.

We used a similar approach to decode sequences occurring within theta cycles while the rat performed the behavioral task. Place cell spiking is concentrated between peaks of the theta rhythm recorded from the hippocampal fissure (Skaggs et al., 1996), so theta cycles were defined as the time between peaks of the theta band-pass filtered fissure LFP. Only theta cycles occurring when the theta-delta ratio was greater than 0.5 standard deviations above baseline were decoded. Only cycles in which at least three cells fired a total of five or more spikes were decoded. Sequences within theta cycles were tested for significance as outlined above. Of 18,550 theta cycles (across all sessions and subjects), 2,040 contained significant sequences (11%).

To demonstrate the efficacy of the decoding algorithm, we constructed a plot of the mean decoded posterior probability distribution for each position on the maze during the run-theta epoch (Fig. 4). Individual examples of significant decoded sequences are shown in Figure 5.

RESULTS

The ratio of forward to backward correlation strength increased during postrun rest. Because forward and backward sequences should produce characteristic patterns of correlations, we computed the cross-correlation of cell pairs that had place fields during the task. We segmented data into epochs (prerun, run-theta, run-LIA, postrun), computed cross-correlograms separately for each, and sorted correlograms by the distance between place fields of the cell pair. Plotted in this way (Fig. 2), forward sequences should produce bands of increased correlation diagonally from the lower-left to the upper-right of the plot. Reverse sequences should result in activity concentrated along the opposite diagonal.

No correlation patterns were apparent in spiking during the pre-run epoch (Fig. 2). The pattern of correlations during the run-theta epoch, however, indicated forward-directed activity on multiple timescales. A broad band of increased correlation spanned the entire 1 s window, due to the sequential firing of cells with place field separations less than $\sim$50 cm. Smaller, forward-directed bands spaced at 120-ms intervals were visible within the region of heightened correlation, due to forward sequences within individual theta cycles. Correlations indicative of forward and backward sequences were present during the run-LIA epoch. Observation of the run-LIA epoch correlogram suggests an X centered on colocalized pairs, indicating the presence of forward and backward firing relationships. The postrun epoch also showed evidence for sequences in both directions, but a stronger correlation in the forward direction was evident, as indicated by the strong forward diagonal.
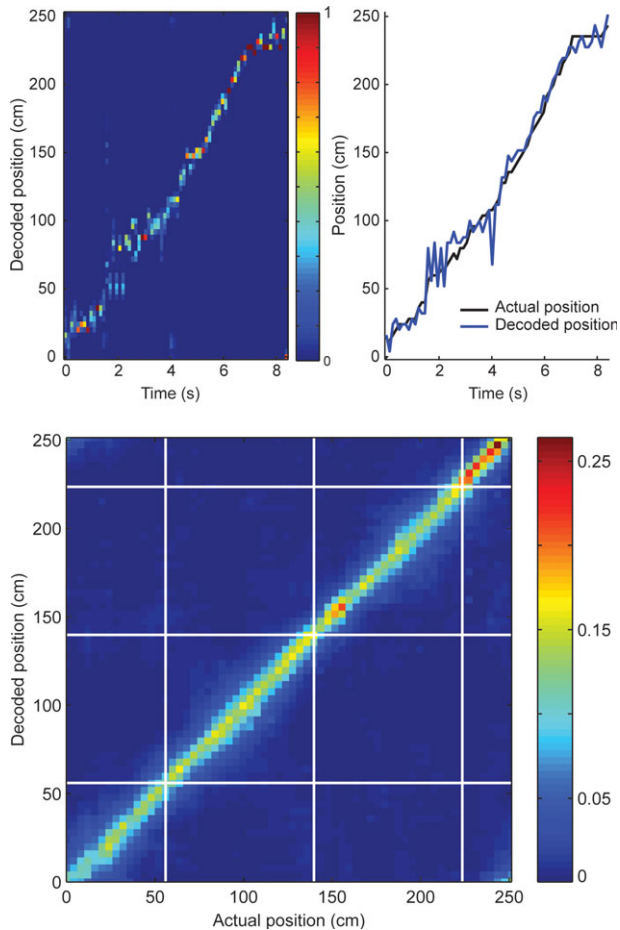
FIGURE 4.   A Bayesian decoding algorithm was used to esti-mate spatial trajectories represented by firing sequences. The top panel shows decoding as a subject runs a trajectory around the track. The peak of the decoded posterior distribution for each time step (top left) matches the animal's position each moment in time. Similarly, decoded position tracks actual location well (top right). The bottom panel displays the mean decoded posterior dis-tribution for each position in space within the run-theta epoch. Food delivery locations are marked with white lines. Decoded probability is concentrated along the diagonal, indicating accurate spatial decoding. [Color figure can be viewed in the online issue, which is available at wileyonlinelibrary.com.]

To quantify the balance of forward and backward activity, we compared the intensity of pixels in forward quadrants (northeast and southwest) of cross-correlograms with pixels in backward quadrants (northwest and southeast; Fig. 3). There were no significant differences in the distributions for the pre-run and run-LIA epochs ($P = 0.69$ and $P = 0.09$, respectively; ranksum test); however, forward correlations were significantly stronger in the run-theta and postrun epochs (both $P < 10^{-10}$; Fig. 3).

We confirmed that correlation patterns were similar across rats by performing the same quantification separately for each subject. Consistent with the grouped data, no differences in forward and backward correlation intensity were observed for the prerun and run-LIA epochs (prerun $P = 0.36$, 0.31, and

0.44; run-LIA $P = 0.07$, 0.19, and 0.17, for rats 1–3, respec-tively; ranksum test) Forward correlation intensity was greater than backward correlation intensity in the run-theta and post-run epochs (all P values for all rats $< 10^{-10}$; ranksum test).

Forward sequences were more prevalent than backward sequences during postrun rest. To more directly assess the prev-alence of forward and backward sequences, we decoded spatial positions represented by sequential spiking (Davidson et al., 2009; Karlsson and Frank, 2009). We applied a one-step Bayesian decoding algorithm (Zhang et al., 1998) with a uni-form spatial prior to ensemble spiking during candidate sequences (defined as times of increased ripple LFP power), producing a time series of probability distributions over space for each event. To determine the direction of sequences, we fit regression lines to the cumulative sum of differences between subsequent decoded positions. We used a shuffling procedure (Karlsson and Frank, 2009) to statistically evaluate decoded representations; sequences unlikely to have arisen by chance ($P < 0.05$) were deemed significant. Because theta sequences fall within cycles of the theta rhythm, we decoded spiking in indi-vidual theta cycles for the run-theta epoch.

In general, the Bayesian decoding algorithm provided an accurate, unbiased estimate of hippocampal ensemble represen-tations. The bulk of the decoded probability distribution matched the rat's actual location during the run-theta epoch (Fig. 4), consistent with veridical place cell representations of position. Examples of significant decoded ripple-associated sequences are shown in Figure 5.

Figure 6 shows histograms of slopes for significant sequences in each epoch. In agreement with the cross-correlation results (Figs. 2 and 3), very few significant sequences were found in the prerun epoch, and sequences during run-theta were pre-dominantly forward (78.5%). Both forward and backward sequences were present in the run-LIA (47.0% forward) and post-run (60.0% forward) epochs.

To statistically describe the balance of forward and backward sequences in each epoch, we used two-tailed signrank tests to ask whether distributions of sequence slopes were significantly different than zero. The balance of forward and backward sequences was not significantly different for the run-LIA epoch ($P = 0.08$, signrank test). However, there were significantly more forward sequences during both the run-theta ($P < 10^{-6}$) and post-run ($P < 10^{-3}$) epochs.

We confirmed that data from individual subjects matched the pattern of results in the grouped data. Considered sepa-rately, the balance of forward and backward sequences did not differ for prerun ($P = 0.36$, 0.15, 0.21 for rats 1–3, respec-tively; signrank test) or run-LIA ($P = 0.15$, 0.17, 0.28 for rats 1–3, respectively; signrank test) epochs for any subjects. How-ever, distribution medians were significantly greater than zero for all subjects in the run-theta epoch (median = 0.06, 0.08, 0.05 for rats 1–3, respectively; all P values for all rats $< 10^{-10}$; signrank test). Similarly, in the postrun epoch, the medians of distributions of sequence slopes were significantly greater than zero for each subject (medians = 0.18, 0.16, 0.13; $P = 0.001$, 0.02, 0.03 for rats 1–3, respectively; signrank test).
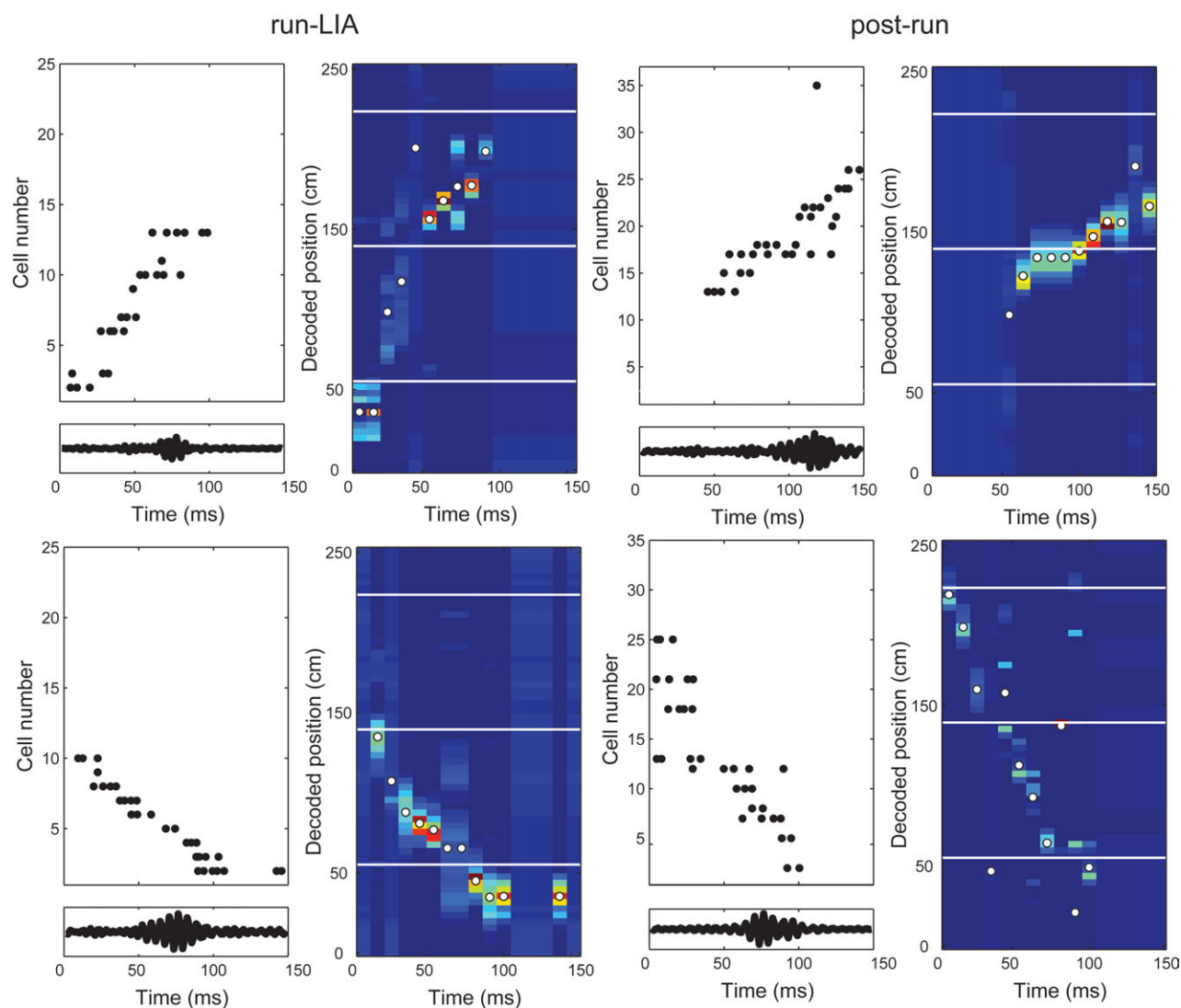
FIGURE 5. Four decoded firing sequences from the run-LIA (first column) and post-run (second column) epochs. The left-hand plot for each sequence shows rasters of place cell spiking. Cells are ordered by the position of their place fields on the maze (cells with multiple fields are plotted at the position of the field with the highest firing rate). Panels below each raster show the ripple band-pass filtered LFP. The right-hand plot for each sequence is the decoded probability distribution, with position on the *y* axis and time on the *x* axis. Food delivery locations are indicated with white lines, and the decoded position at each time step containing at least one spike is marked with a white dot. [Color figure can be viewed in the online issue, which is available at wileyonlinelibrary.com.]

DISCUSSION

Here, we used two approaches to measure the direction of hippocampal sequences over four behavioral/physiological conditions. Our analyses found that when the hippocampus was in the LIA network state, during either brief pauses in on-going behavior or during postbehavior rest, sequential place cell representations were expressed. However, forward and backward sequences occurred in different proportions during on-line and off-line states. During on-line pausing, both forward and backward sequences were observed, consistent with previous findings from Diba and Buzsaki (2007) and Davidson et al. (2009). As reported in Gupta et al. (2010), forward and backward sequences were equally prevalent during the run-LIA epoch. In con-

trast, during postrun rest, forward sequences were more common than backward sequences, consistent with early findings from Skaggs and McNaughton (1996), Nadasdy et al. (1999), and Kudrimoti et al. (1999). Our results unify these seemingly conflicting reports by showing that the reported discrepancies are due to fundamental differences in SWR reactivation patterns depending on sleep/wake state, not methodological differences or variability in subjects across experiments.

The findings presented here have implications for existing models of hippocampal sequence generation. We report the first (to our knowledge) demonstration of backward sequences during an off-line state. This finding is perhaps not surprising, given the prevalence of backward sequences during awake pausing (Foster and Wilson, 2006; Diba and Buzsaki, 2007;
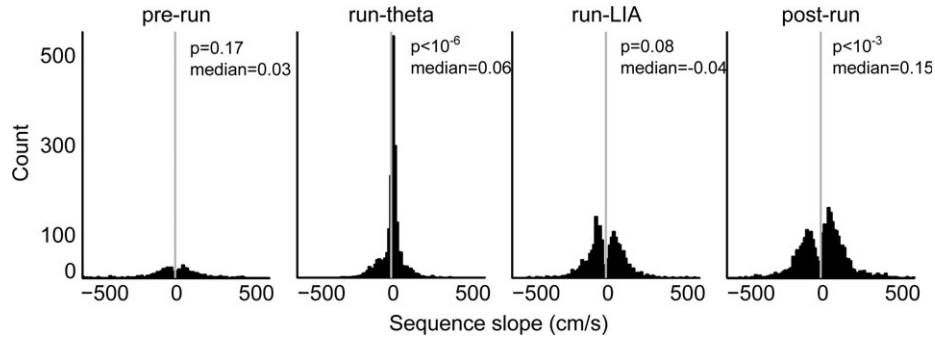
FIGURE 6.   To measure sequence direction we fit regression lines to the cumulative sum of differences between consecutive decoded positions. Forward sequences have positive slopes, while backward sequences have negative slopes. Histograms of sequence slopes are shown, with a vertical grey line at zero. To assess the bal-ance of forward and backward sequences, we used a sign-rank test to test if medians of the distributions were significantly different than zero. The medians of distributions were not different than zero for the pre-run and run-LIA conditions. However, medians were significantly greater than zero during the run-theta and post-run epochs.

Davidson et al., 2009; Gupta et al., 2010). Indeed, at least one model of hippocampal replay explicitly predicted backward replay within SWRs during slow-wave sleep (Molter et al., 2006). We attempted to isolate only periods of slow-wave sleep in the prerun and postrun epochs. However, given the similarity in the behavior and neurophysiology of slow-wave sleep and awake quiescence, it is possible that sequences detected during these epochs derive from both awake and sleep LIA. In future studies, electromyogram (EMG) recordings (e.g., Ego-Stengel and Wilson 2010) could be used to distinguish between these states. In any case, considered along with other recent findings (Davidson et al., 2009; Karlsson and Frank, 2009; Gupta et al., 2010), the expression of reverse sequences during the postrun epoch challenges models in which such events are initiated by a slowly decaying excitability trace lingering in recently active neurons (Buzsaki, 1989; Foster and Wilson, 2006; Csicsvari et al., 2007; O'Neill et al., 2008).

The shift in the balance of backward and forward sequences between the run-LIA and postrun epochs might reflect changes in the nature of information processing in the hippocampus. During behavior, in addition to memory consolidation, the hippocampus could support other, more integrative processes via backward replay, such as reinforcement learning (Foster and Wilson, 2006), novel trajectory construction (Samsonovich and Ascoli, 2005; Molter et al., 2007; Gupta et al., 2010) or spatial working memory (Jadhav et al., 2012). Forward sequences in online states could support immediate consolidation of ongoing behavior, memory recall, or yet undescribed processes (Carr et al., 2011). In conjunction, backward and forward sequences during behavior could aid the development of a Tolmanian cognitive map, allowing animals to use complicated spatial behaviors like shortcuts (Molter et al., 2007; Derdikman and Moser, 2010; Gupta et al., 2010).

The increase in forward sequences during postbehavior sleep might reflect consolidation of experience gained during task performance (Marr, 1971; Buzsaki, 1989; Sutherland and McNaughton, 2000). Using electrical stimulation to disrupt patterned firing during SWRs in sleep following behavior leads to learning deficits (Girardeau et al., 2009; Ego-Stengel and Wilson, 2010), suggesting consolidation is at least one of the roles fulfilled by off-line sequential reactivation. However, because this manipulation did not discriminate forward and backward sequences, it is not clear whether disruption of sequences in one direction in particular impaired learning.

Hippocampal sequences during sleep could also fulfill functions other than consolidation. Stringing together segments of forward and backward trajectories could lead to the formation of novel associations between disparate pieces of experience, possibly explaining the relationship between sleep and insight (Wagner et al., 2004). Off-line sequences could also assist cognitive restructuring processes like schema formation, abstraction, or integration of new information into existing representations (Samsonovich and Ascoli, 2005; Wamsley and Stickgold, 2010; Buhry et al., 2011; Lewis and Durrant, 2011).

Although questions remain about the exact functional role or roles that hippocampal sequences fulfill, the data presented here and other recent findings (Carr et al., 2011) suggest sequences in the hippocampus might play a more nuanced role beyond rote repetition of previous experience for consolidation.

Acknowledgments

REFERENCES

Buhry L, Azizi AH, Cheng S. 2011. Reactivation, replay and preplay: How it might all fit together. Neural Plasticity 2011:1–11.

Buzsaki G. 1989. Two-stage model of memory trace formation: A role for "noisy" brain states. Neuroscience 31:551–570.

Buzsaki G, Leung LW, Vanderwolf CH. 1983. Cellular bases of hippocampal EEG in the behaving rat. Brain Res 287:139–171.

Carr MF, Jadhav SP, Frank LM. 2011. Hippocampal replay in the awake state: A potential substrate for memory consolidation and retrieval. Nat Neurosci 14:147–153.

Cheng S, Frank LM. 2008. New experiences enhance coordinated neural activity in the hippocampus. Neuron 57:303–313.

Cohen NJ, Eichenbaum H. 1993. Memory, Amnesia, and the Hippocampal System. Cambridge, MA: MIT Press.

Csicsvari J, Hirase H, Czurko A, Buzsaki G. 1999. Oscillatory coupling of hippocampal pyramidal cells and interneurons in the behaving rat. J Neurosci 19:274–287.

Csicsvari J, O'Neill J, Allen K, Senior T. 2007. Place-selective firing contributes to the reverse-order reactivation of CA1 pyramidal cells during sharp waves in open-field exploration. Eur J Neurosci 26:704–716.

Davidson TJ, Kloosterman F, Wilson MA. 2009. Hippocampal replay of extended experience. Neuron 63:497–507.

Derdikman D, Moser MB. 2010. A dual role for hippocampal replay. Neuron 65:582–584.

Diba K, Buzsaki G. 2007. Forward and reverse hippocampal place-cell sequences during ripples. Nat Neurosci 10:1241–1242.

Dragoi G, Buzsaki G. 2006. Temporal encoding of place sequences by hippocampal cell assemblies. Neuron 50:145–157.

Ego-Stengel V, Wilson MA. 2010. Disruption of ripple-associated hippocampal activity during rest impairs spatial learning in the rat. Hippocampus 20:1–10.

Foster DJ, Wilson MA. 2006. Reverse replay of behavioral sequences in hippocampal place cells during the awake state. Nature 440:680–683.

Foster DJ, Wilson MA. 2007. Hippocampal theta sequences. Hippocampus 17:1093–1099.

Girardeau G, Benchenane K, Wiener SI, Buzsaki G, Zugaro MB. 2009. Selective suppression of hippocampal ripples impairs spatial memory. Nat Neurosci 12:1222–1223.

Gupta AS, van der Meer MAA, Touretzky DS, Redish AD. 2010. Hippocampal replay is not a simple function of experience. Neuron 65:695–705.

Gupta AS, van der Meer MAA, Touretzky DS, Redish AD. Segmentation of spatial experience by hippocampal theta sequences. Nature Neuroscience doi: 10.1038/nn.3138.

Hasselmo ME. 1993. Acetylcholine and learning in a cortical associative memory. Neural Computation 5:32–44.

Hirase H, Leinekugel X, Czurko A, Csicsvari J, Buzsaki G. 2001. Firing rates of hippocampal neurons are preserved during subsequent sleep episodes and modified by novel awake experience. Proc Natl Acad Sci 98:9386–9390.

Hoffmann KL, McNaughton BL. 2002. Coordinated reactivation of distributed memory traces in primate neocortex. Science 297:2070–2073.

Jackson JC, Johnson A, Redish AD. 2006. Hippocampal sharp waves and reactivation during awake states depend on repeated sequential experience. J Neurosci 26:12415–12426.

Jadhav SP, Frank LM. 2009. Reactivating memories for consolidation. Neuron 62:745–746.

Jadhav SP, Kemere C, German PW, Frank LM. 2012. Awake hippocampal sharp-wave ripples support spatial memory. Science 336:1454–1458.

Karlsson MP, Frank LM. 2009. Awake replay of remote experiences in the hippocampus. Nat Neurosci 12:913–918.

Kudrimoti HS, Barnes CA, McNaughton BL. 1999. Reactivation of hippocampal cell assemblies: Effects of behavioral state, experience, and EEG dynamics. J Neurosci 19:4090–4101.

Lansink CS, Goltstein PM, Lankelma JV, McNaughton BL, Pennartz CMA. 2009. Hippocampus leads ventral striatum in replay of place-reward information. PLoS Biol 7:e1000173.

Lee AK, Wilson MA. 2002. Memory of sequential experience in the hippocampus during slow wave sleep. Neuron 36:1183–1194.

Lewis PA, Durrant SJ. 2011. Overlapping memory replay during sleep builds cognitive schemata. Trends Cogn Sci 15:343–351.

Marr D. 1971. Simple memory: A theory of archicortex. Phil Transact Roy Soc Lond 262:23–81.

Maurer AP, Burke SN, Lipa P, Skaggs WE, Barnes CA. 2011. Greater running speeds result in altered hippocampal phase sequence dynamics. Hippocampus 22:737–747.

Molter C, Sato N, Salihoglu U, Yamaguchi Y. 2006. How reward can induce reverse replay of behavioral sequences in the hippocampus. In: King I, Wang J, Chan LW, Wang D, editors. Neural Information Processing, Vol. 4232 of Lecture Notes in Computer Science. Berlin/Heidelberg: Springer. pp 1–10.

Molter C, Sato N, Yamaguchi Y. 2007. Reactivation of behavioral activity during sharp waves: A computational model for two stage hippocampal dynamics. Hippocampus 17:201–209.

Nadasdy Z, Hirase H, Czurko A, Csicsvari J, Buzsaki G. 1999. Replay and time compression of recurring spike sequences in the hippocampus. J Neurosci 19:9497–9507.

O'Keefe J. 1976. Place units in the hippocampus of the freely moving rat. Exp Neurol 51:78–109.

O'Keefe J, Dostrovsky J. 1971. The hippocampus as a spatial map. Preliminary evidence from unit activity in the freely moving rat. Brain Res 34:171–175.

O'Keefe J, Nadel L. 1978. The Hippocampus as a Cognitive Map. Oxford: Clarendon Press.

O'Keefe J, Recce M. 1993. Phase relationship between hippocampal place units and the EEG theta rhythm. Hippocampus 3:317–330.

O'Neill J, Senior TJ, Allen K, Huxter JR, Csicsvari J. 2008. Reactivation of experience-dependent cell assembly patterns in the hippocampus. Nat Neurosci 11:209–215.

Redish AD. 1999. Beyond the Cognitive Map: From Place Cells to Episodic Memory. Cambridge MA: MIT Press.

Redish AD, Ekstrom A. Hippocampus and related areas: What the place cell literature tells us about cognitive maps in rats and humans. In: Handbook of spatial cognition, Waller D and Nadel L, Eds. APA Books (in press).

Redish AD, Touretzky DS. 1998. The role of the hippocampus in solving the Morris water maze. Neural Computation 10:73–111.

Samsonovich AV, Ascoli GA. 2005. A simple neural network model of the hippocampus suggesting its pathfinding role in episodic memory retrieval. Learn Memory 12:193–208.

Schmidt R, Diba K, Leibold C, Schmitz D, Buzsaki G, Kempter R. 2009. Single-trial phase precession in the hippocampus. J Neurosci 29:13232–13241.

Singer AC, Frank LM. 2009. Rewarded outcomes enhance reactivation of experience in the hippocampus. Neuron 64:910–921.

Skaggs WE, McNaughton BL. 1996. Replay of neuronal firing sequences in rat hippocampus during sleep following spatial experience. Science 271:1870–1873.

Skaggs WE, McNaughton BL, Wilson MA, Barnes CA. 1996. Theta phase precession in hippocampal neuronal populations and the compression of temporal sequences. Hippocampus 6:149–173.

Sutherland GR, McNaughton BL. 2000. Memory trace reactivation in hippocampal and neocortical neuronal ensembles. Curr Opin Neurobiol 10:180–186.

Vanderwolf CH. 1969. Hippocampal electrical activity and voluntary movement in the rat. Electroencephalography Clin Neurophysiol 26:407–418.

Vanderwolf CH. 1971. Limbic-diencephalic mechanisms of voluntary movement. Psychological Rev 78:83–113.

Wagner U, Gais S, Haider H, Verleger R, Born J. 2004. Sleep inspires insight. Nature 427:352–355.

Wamsley E, Stickgold R. 2010. Dreaming and offline memory processing. Curr Biol 20:1010–1013.

Wikenheiser AM, Redish AD. 2011. Changes in reward contingency modulate the trial to trial variability of hippocampal place cells. J Neurophysiol 106:589–598.

Wilson MA, McNaughton BL. 1994. Reactivation of hippocampal ensemble memories during sleep. Science 265:676–679.

Zhang K, Ginzburg I, McNaughton BL, Sejnowski TJ. 1998. Interpreting neuronal population activity by reconstruction: Unified framework with application to hippocampal place cells. J Neurophysiol 79:1017–1044.